26th ABCM International Congress of Mechanical Engineering
November 22-26, 2021. Florianópolis, SC, Brazil

COB-2021-1176
ALUMINA COATINGS ON STAINLESS STEEL AND HIGH-DENSITY GRAPHITE SUBSTRATES OBTAINED BY PLASMA SPRAY PROCESS

Roberson José da Silva
Tiago Moreira Bastos Campos
Felipe de Souza Miranda
Homero Santiago Maciel
Gilberto Petraconi Filho
Instituto Tecnológico de Aeronáutica, São José dos Campos, SP, Brasil
roberson123@gmail.com, moreiratiago22@gmail.com, mirannda.fs@gmail.com, odairtur@gmail.com, petrafilho@gmail.com

Abstract. *Aeronautical and aerospace applications for devices such as turbines and rocket engines require resistance to extreme environmental conditions for some materials, which are used. Metallic materials resistant to oxidation, when used in extreme environments such as turbine combustion chambers, at high temperatures, may be more susceptible to ablation and chemical attacks. Graphite, which is commonly used in rocket engine throats and nozzles, has thermal and mechanical properties that remain at high temperatures, but oxidation can limit its applicability. Refractory ceramics are known for their resistance to chemical and thermal attack environments. A ceramic coating can be used as a way to complement the properties of these materials, protecting them from oxidative and ablative processes at high temperatures. Thus, the objective of this work is to study the ceramic coating on stainless steel and graphite substrates by using a thermal spray plasma process with ceramic powder. This work presents the experimental studies performed by using a tornado-type thermal plasma torch, working at a power of 30 kW, at 105 A. In this condition, the hot gas plasma generated at 5200 ºC melts the alumina powder of 70-200 mesh, which is sprayed on the substrate. The spraying of the powder in the plasma jet was performed by a vibrating powder feeder with a powder flow rate at 5-10 g/min and a flow rate of carrying gas at 5 SLPM. The powder melted in the thermal spray was deposited on substrates of AISI 304 stainless steel and graphite. The application of the coating on the substrates was performed in two ways, i.e., fixed and dynamic. The fixed application was performed with the substrate positioned at an optimized distance on the axis of the spray jet and obtained a deposition peak of 60 µm on stainless steel in the region of the spray focus. On carbon, the thickness was similar but irregular. The dynamic application was performed using an automatic device, developed to apply rotation and horizontal movement to the substrates, performing an area sweep with the jet on its surface to obtain a homogeneous coating. The formation of a uniform alumina coating on both stainless steel and graphite was observed by SEM and EDS, with a thickness of 40-50 µm on the stainless steel substrate and 80-150 µm on the graphite substrate with relatively greater uniformity than in the deposition with fixed positioning. These results show that this technique can be used to obtain refractory coatings on these materials.*

Keywords: *thermal spray, plasma spray, alumina coating, powder, aerospace*

1. INTRODUCTION

Environmental protection of graphite-based and C/C components against the high-temperature ablative environment is critical for reentry vehicles, ablative thrusters, and other applications (Miranda et al., 2017). Its high strength and exceptional fracture toughness, combined with its refractory properties, low density, high resistance to erosion, corrosion and wear make this material ideal for applications in structural components subjected to high temperatures, such as turbines and atmospheric reentry vehicles (Miranda et al., 2020). When used in inert atmospheres or a vacuum, C/C composites maintain their properties at temperatures above 2000 °C (Webster et al., 1996). However, in the conditions of oxidizing environments at high temperatures, carbonaceous materials undergo intense degradation due to the high catalytic reaction between carbon and oxygen, making their use in aerospace devices difficult and often impossible (Kim et al., 2005). This problem can be overcome by depositing thermal/environmental barrier coatings to protect against oxidation, loss of mass, and to enhance the mechanical properties of the substrate.

Coatings that protect the substrate against thermal oxidation, failures caused by high temperatures or thermal flow are classified as Environmental Barrier Coatings (EBC) (Ando et al., 2005; Engel & Kickelbick, 2014; Lee, 2000). The EBCs coatings must withstand reactive environments, having low oxygen permeability (so that it is not transported to the substrate) and, finally, being chemically compatible with the substrate (Lee, 2000). For effective protection, the deposition or formation of oxides in the coating, such as Al_2O_3, SiO_2, ZrO_2 among others, is desirable (Miranda et al., 2017).

The objective of this work is to study the ceramic coating on stainless steel and graphite substrates by using a thermal spray plasma process with ceramic powder and presenting the experimental studies using a tornado-type thermal plasma torch, working at a power of 30 kW, at 105 A. The deposition of the coatings is made in two methods, which are, static and dynamic. The static deposition was performed with the substrate positioned at a fixed distance on the axis of the spray jet, and the dynamic deposition was made using a rotary and horizontal movement sample holder, aiming to sweep the substrate with the jet on its surface to obtain a homogeneous coating. The formation of a uniform alumina coating on both stainless steel and graphite was observed by SEM and EDS, showing that this technique can be used to obtain refractory coatings on these materials.

2. MATERIALS AND METHODS

2.1 Materials

The substrates used in this work were AISI 304 stainless steel and high-density graphite (widely used in the aerospace sector). Figure 1 shows the real image and the specifications of the substrates used in the depositions.

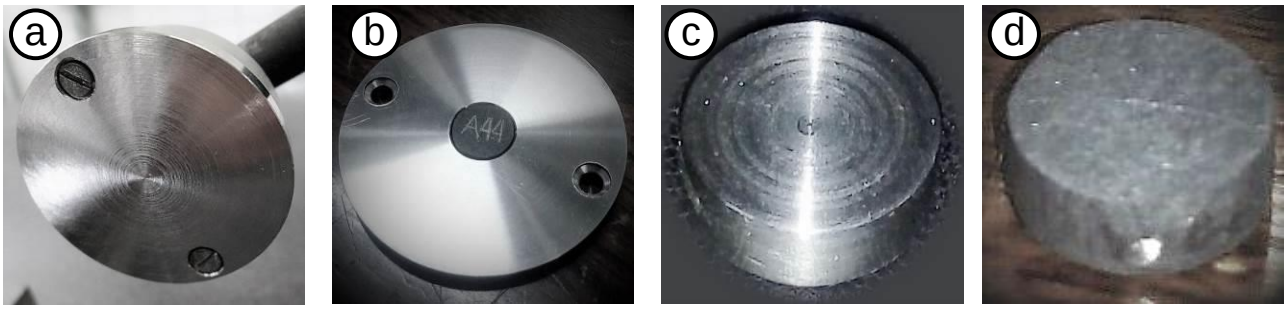

Substrate	Material	Diameter (mm)	Thickness (mm)	Type of Deposition Process [1]
a	stainless steel	45	4	Static
b	graphite [2]	10	4	static
c	stainless steel	10	4	rotative
d	stainless steel	10	4	angular sweep

[1] sample holder positioning [2] graphite substrate inserted in type “a” disc

Figure 1. Substrates used in each type of deposition process

In Figure 2, images of the powder used in the depositions are presented (a). It is an alumina powder with a particle size of 70-210 µm. As shown in the micrographs, the particles have a spherical morphology (b and c), they are formed by platelets agglomerated with a diameter between 1-5 µm and 1 µm thick (d). The average particle size of these agglomerates, about 100 µm, makes it reach enough kinetic energy to penetrate the core of the plasma plume (highest temperature region), helping in the absorption of thermal energy and consequently a greater number of molten particles that will compose the coating. On the other hand, the fact that these particles are agglomerates of smaller particles (platelets) rather than solid bodies, also contributes to the fusion of the powder as they increase the surface area of the particle allowing greater absorption of thermal energy.

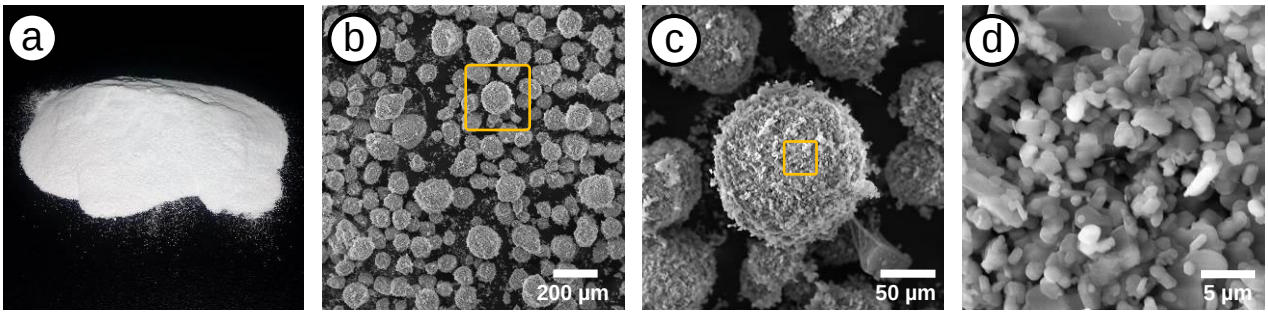

Figure 2. Alumina powder used for the coatings

2.2 Plasma spray system

The plasma torch used is a tornado type. It works using air as the working gas at a flow rate of 90 L/min and is supplied with 30 kW of energy (105 A, 285 V). In this condition, in the 6 mm outlet nozzle of the plasma torch, a supersonic plasma jet with a specific enthalpy of 11 MJ/kg is generated, with a temperature of 5100 °C (Pfender et al., 1994). In these conditions the system promoting the fusion of the alumina powder, and a velocity of about 500 m/s for the molten particles. The injection of powder into the plasma jet was achieved with a Tekna model PFV 101 vibrational powder feeder (Silva et al., 2019a). In this work, 3 different processes were used for alumina deposition, according to the positioning of the substrate in relation to the plasma jet: static, rotary and angular sweep.

In the static positioning deposition process (Figure 3), the substrate was fixed to an aluminum base, attached to the end of a cooled copper arm. This arm functions as a lever that suspends the sample in front of the plasma jet at a programmed distance in an X-Y system where the base of the lever is attached. The powder spray focus on the substrate is set at the center of the substrate with the mechanical alignment of the lever system and the plasma torch shaft. After turning on, stabilizing the torch and injecting powder into the plasma jet, the substrate is positioned in front of the jet. Then it stays there for a programmed time, receiving the alumina powder particles that are pulverized and melted in the plasma jet. At the end of the programmed time, the arm descends, removing the sample from the front of the plasma jet and the X-Y system returns to the initial position (Silva et al., 2019a). The deposition parameters that were used for each substrate are shown in Figure 3.

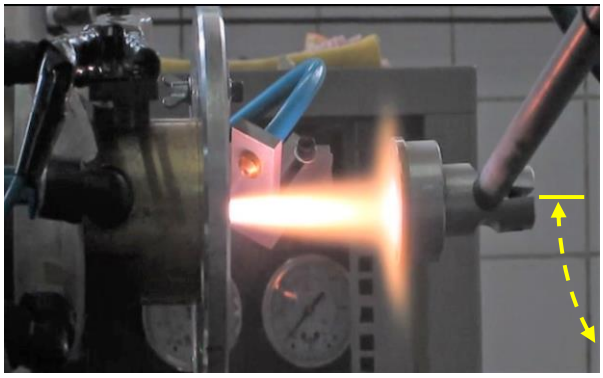

Parameters	Substrate	
	Stainless Steel	Graphite
powder flow rate	2,6 - 3,3 g/min	4 – 6 g/min
powder carried gas flow rate	5 SLPM	5 SLPM
substrate-torch distance	65 mm	65 mm
time per deposition cycle	4 s	4 s (1)
number of deposition cycles	8	16

(1) 1ª and 2ª deposition at 10 s and 3ª and 4ª at 5 s.

Figure 3. Deposition with static positioning

Deposition with rotary positioning is shown in Figure 4-a. For this process of deposition, an automatic actuation system was developed to apply movements of axial displacement (1) and rotation (2) in an axis. A disc-shaped stainless steel sample holder with 70 mm in diameter was fixed at the end of this axis (Figure 4-b). Up to 6 substrates with the dimensions defined in Figure 1-c are fixed in this sample holder. With the combined movements during deposition, the spray focus performs a sweep on the sample holder surface in order to deposit a homogeneous coating ring. As shown in Figure 4-c, the red lines indicate the sweep of the spray focus during the axial advance and the green lines indicate the return. The actuation system can be programmed in axial speed, range of axial displacement and rotational speed, enabling the optimization of deposition. The deposition parameters used are shown in Figure 4.

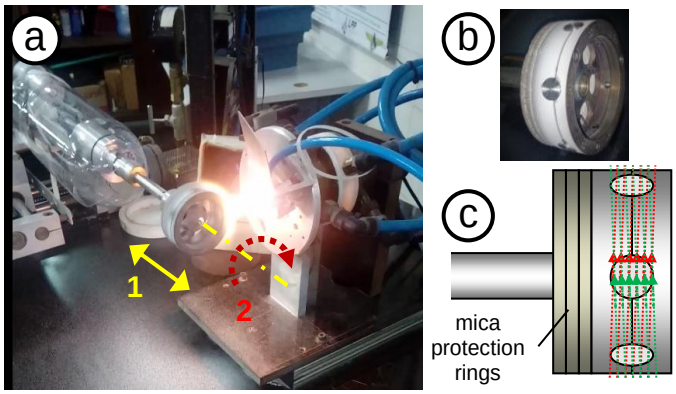

Parameters	Value
powder flow rate	6 – 9 g/min
powder carried gas flow rate	5 SLPM
substrate-torch distance	65 mm
sample holder rotational speed	100 rpm
sample holder axial displacement	± 5 mm
axial speed	3 mm/s
time per deposition cycle	77 s
number of deposition cycles	3

Figure 4. Deposition with rotary positioning

With the rotary positioning, it was not possible to successfully coat the graphite substrate. These substrates require a higher concentration of energy to obtain a coating than stainless steel substrates. To solve this issue, an angular sweep

mode was added to the automatic actuation system to perform a sweeping motion of an angular range covering only the area around the substrate (Figure 5-a). Now, defining the angular displacement range, angular velocity, axial displacement range and axial velocity, the spray focus will sweep the specimen surface in zig and zag motions, as shown in Figure 5-b. To perform this sweep, as showed in Figure 5-b, it was necessary to include in this actuation mode, a synchronism control between the movements of the axial displacement and angular sweep. A smaller sample holder was also developed, with a diameter of 24 mm and a forecast for only 3 substrates at a time, as shown in the detail in Figure 5-c. This sample holder can also be used for rotary positioning mode on up to 3 stainless steel samples, however, deposition is performed on only one sample at a time in angular sweep mode. The deposition parameters used are shown in Figure 5.

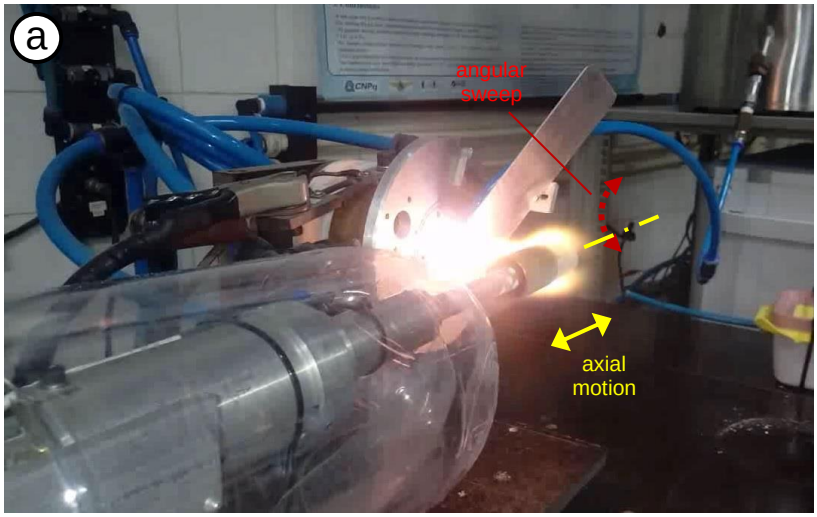

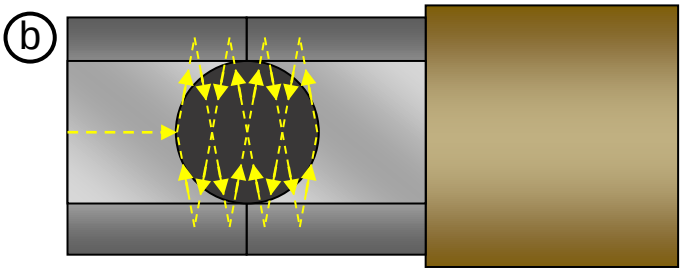

Parameters	Value
powder flow rate	6 – 9 g/min
powder carried gas flow rate	5 SLPM
substrate-torch distance	65 mm
sample holder angular range	40 °
sample holder angular speed	40 °/s
sample holder axial displacement	± 5 mm
axial speed	2,5 mm/s
time per deposition cycle	8 s (1)
number of deposition cycles	6

(1) Effective time of the spray focus sweep on the substrate. For the total time of plasma incidence in the sampler, consider adding 2.5 s of movement of the spray focus until reaching the substrate.

Figure 5. Deposition with sweep angular positioning

3. RESULTS

3.1 Plasma spray deposition process

Figure 6 shows the result of the coating obtained by using static positioning in the stainless steel substrate (a) and the respective characteristic coating profile (b)(bell-shaped). The profile measurement was obtained using a mechanical profilometer (model P7 Stylus Profiler from KLA Tencor). Visually, cracks in the coating are not noticeable; however, the profilometry reveals a discontinuity in the peak region indicating a rupture in this region, which may have been

generated by non-fused particles overlapping or during the cooling cycles, due to the difference in the thermal expansion coefficient between the metallic substrate and the ceramic coating (Silva et al., 2019b).

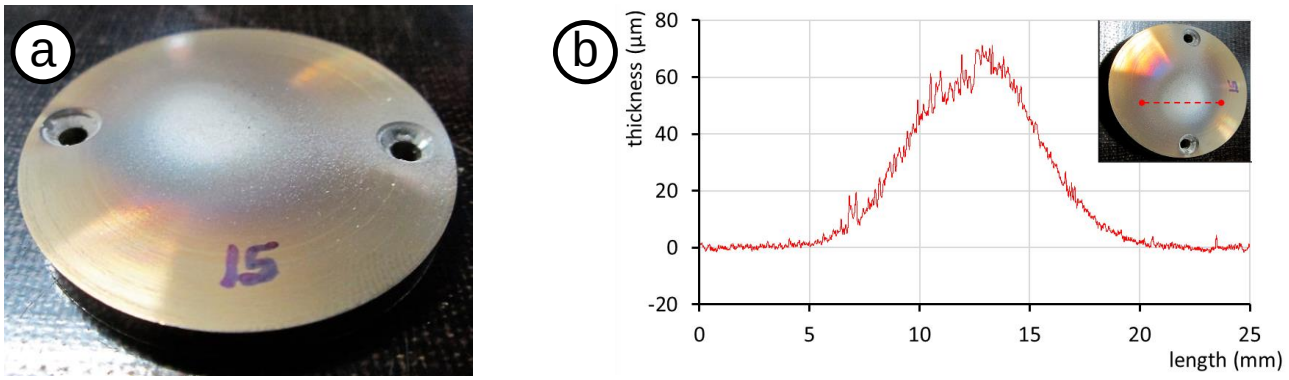

Figure 6. Stainless steel substrate coating by using static positioning

Figure 7 shows the evolution of deposition cycles (d_1 to d_{16}), by using static positioning, that was performed on a graphite substrate. In d_1 and d_2 it is possible to verify that the deposition only takes place on the inner edge of the stainless steel support. An evolution of ablative process is observed on the graphite substrate, without showing significant alumina coating. After reducing the deposition time from 10 to 5 s, in d_3 it is possible to verify a start of coating on the substrate center. Repeating the process until d_7 and reducing the deposition time to 4 s from d_5 onwards, there was an increase in the thickness of the coating in the center of the substrate, however, at its edges, the ablation process persists, evidencing the action of two concurrent processes: deposition and ablation. The deposition process overcomes ablation only in the center region of incidence of the spray jet. From d_8, the spray focus was mechanically aligned to a region lower than the substrate and the deposition cycles were repeated until d_{13}. In d_{11}, a second coating spot is already thicker with an area equivalent to the first coating spot. The persistence of the first coating spot indicates a certain resistance to thermal ablation provided by alumina. However, from d_{12}, the ablative process on the first coating spot becomes evident with the reduction of coated area and it is almost completely removed after d_{13}. In d_{14} to d_{15} depositions, the spray focus was aligned to coat the just detached area. At d_{16} the spray focus was aligned to coat the area between the two overlay spots. The final result is shown in sample A44 without the metallic support. The sample presented a coating on about 80% of the surface. Although irregular, it presented a thick coating (in the order of tenths of a millimeter) and adhered to the substrate. This experiment showed that it is possible to coating larger areas by shifting the spray focus as long as they are understood as limitations imposed by the competition between the deposition and thermal ablation processes.

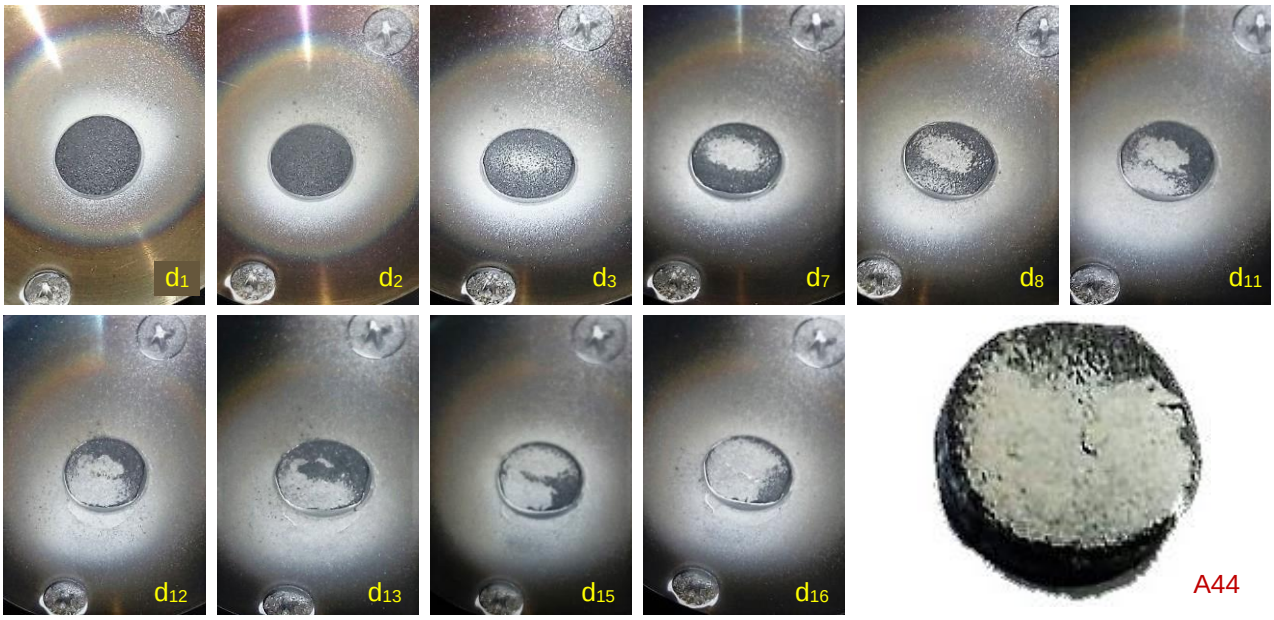

Figure 7. Graphite substrate coating by using static positioning

Figure 8 shows the alumina coating that was obtained by using rotary positioning on stainless steel samples after 3 deposition cycles. It is possible to verify that a homogeneous coating was obtained, both in the substrate samples (b) and in the fixation disk of sample (a), also made of stainless steel.

Figure 8. Stainless steel substrate coating by using rotary static positioning

Figure 9 shows the alumina coating, obtained by using angular sweep positioning on the graphite substrate to 6 deposition cycles (d_1 to d_6). In d_1 coating occurs only at the upper edge of the substrate. In d_2 to d_4, the spray focus is being aligned down, towards the center of the substrate. On d_4 and d_5, you can see that the coating fills almost the entire surface of the substrate, concentrating on a horizontal line in the middle of the substrate and decreasing towards the upper and lower edges. Only a small portion of about 5% of the area remains uncoated at the bottom of the substrate at d_5. At d_6, a proportional increase in coating thickness was observed, but the ablative process leaves about 15% of the surface uncoated at the lower end of the substrate. The coated part of the substrate presented a more homogeneous coating than that observed with deposition by static positioning. This shows that angular scan positioning is a viable solution for performing coating on a graphite substrate. This process promotes the spreading of the coating on the substrate and, at the same time, concentrates enough energy to make the coating viable.

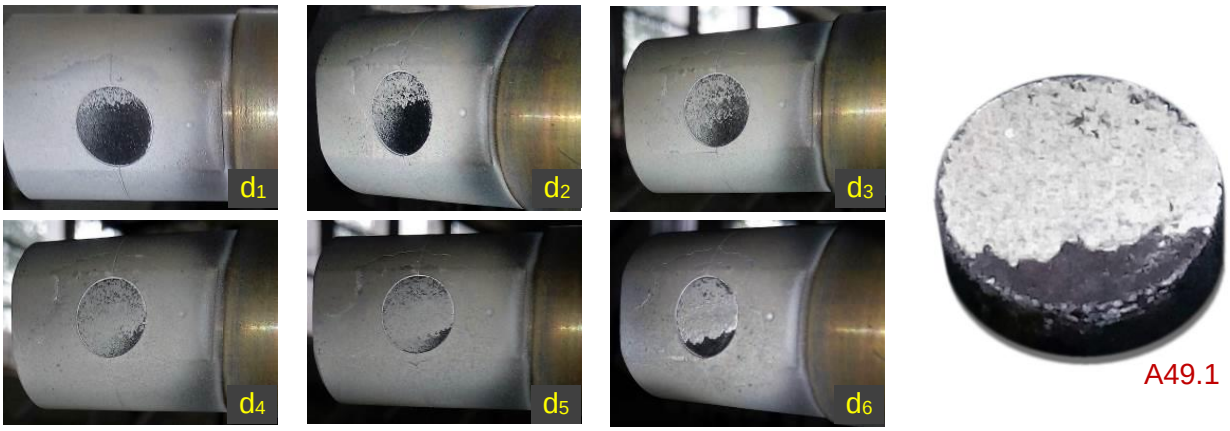

Figure 9. Graphite substrate coating by using angular sweep positioning

3.2 Morphology and structure of the coatings

Figure 10 shows micrographs of the alumina-coated stainless steel substrate by using rotary positioning. The images “a” and “b” show that the coating has a homogeneous distribution and does not present large accumulations or valleys. In “c” it is possible to verify in detail its microstructure formed by stacking splats of fused alumina, characteristic of thermal spray deposition. The image in “d” shows the sample in cross-section. The difference in shade is due to the use of the SEM's backscattered electrons feature, which presents a lighter shade for higher density phases, which allows a better contrast in the identification of the coatings. The darkest phase is formed by the resin. Two bubbles that formed in the sample embedding process during resin curing are seen in this phase. The lighter phase is formed by the metallic substrate. At the interface, in a halftone band, it is possible to identify the alumina coating, which extends in constant thickness across the surface of the sample, presenting slight undulations. In "e", The lightest spots appearing in the coating phase are copper particles generated by the wear of the plasma torch electrodes (as will be shown in the EDS analysis). In “f” it is possible to verify that the thickness of the coating obtained was around 40-50 µm. These results show that the

rotary positioning deposition provided a porous alumina coating, adhered to the stainless steel substrate. The coating showed a constant thickness profile that could be controlled as a function of deposition time or the number of deposition cycles.

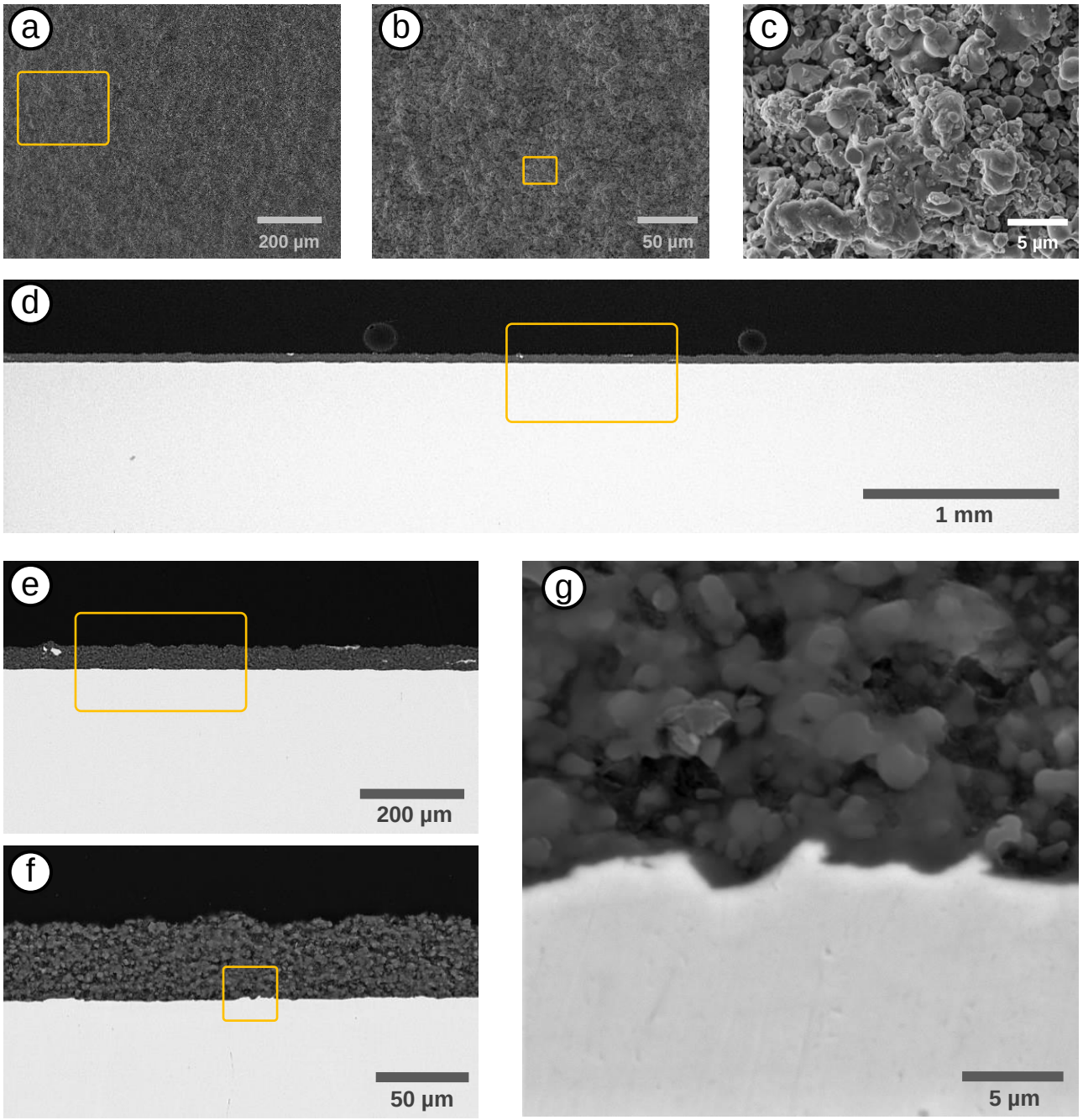

Figure 10. Micrography of sample A49.1 – alumina coating on stainless steel substrate by using rotative positioning

Figure 11-a and “b” show a surface of coating with peaks and valleys more pronounced than in the stainless steel sample in figure 10. The microstructure showed in "c" is determined by the stacking fused alumina splats, similar to figure 10. In the cross-section of the sample, image "d", it is possible to identify 3 phases: the upper darker phase of the resin, the lighter phase, referring to the coating and the lower, also dark, of the graphite substrate. In the graphite phase, it is possible to verify the existence of pores, characteristic of the manufacture of this material. The coating thickness is more constant on the right, towards the center of the sample, and more irregular on the left, towards the edge. The increase in irregularity can be attributed to the concurrent action of the ablative process, verified during depositions on graphite substrates. In “e”, it can be seen that the coating reached thicknesses of around 80 - 150 µm. In “f” it was verified that the fused alumina penetrates the cracks and exposed pores of the graphite and thus promotes the adhesion of the coating to

the substrate. The characteristic porosity of graphite, in this case, contributes to the adhesion of the coating, promoting points for mechanical overlapping.

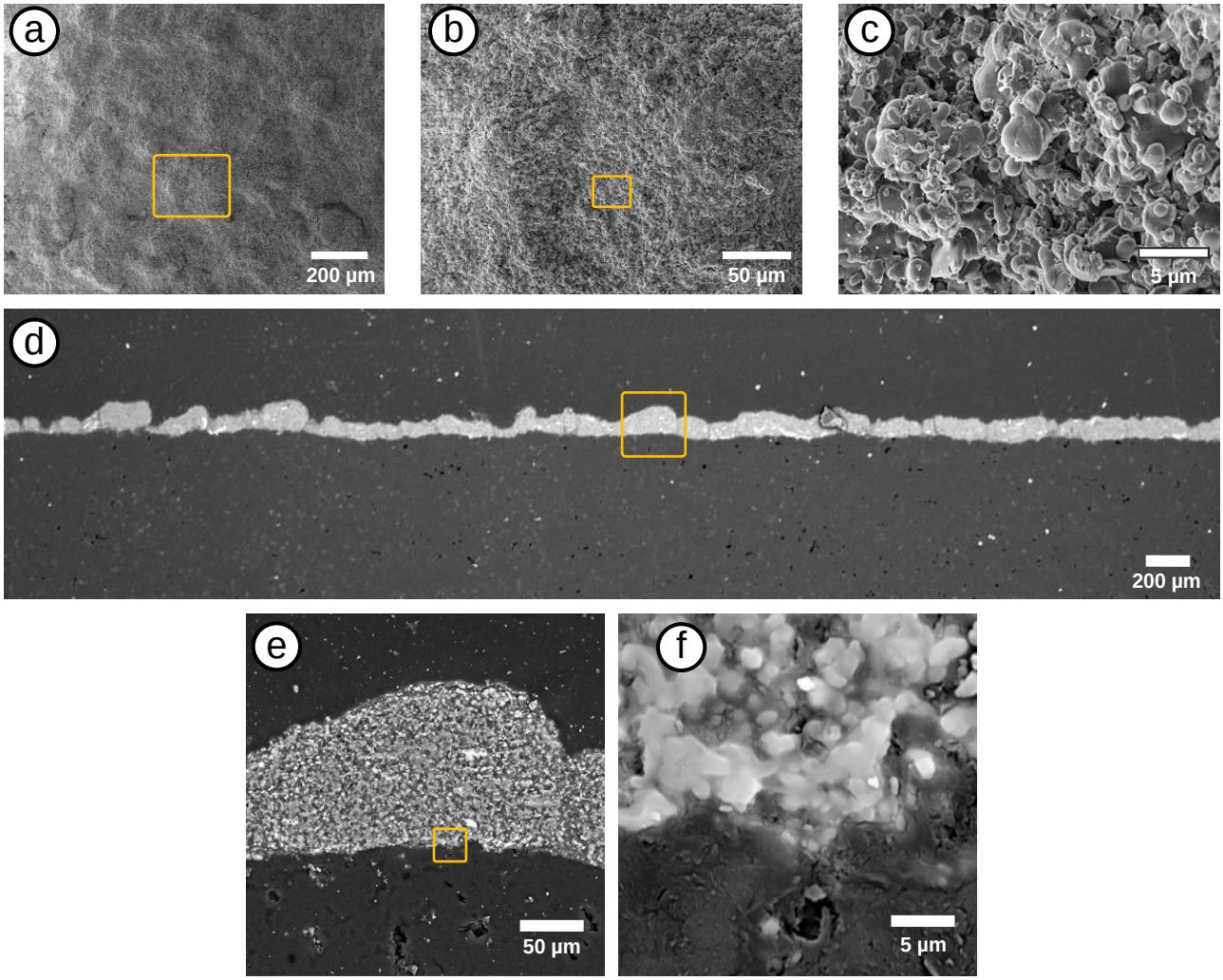

Figure 11. Micrography of sample A49.1 – alumina coating on graphite substrate by using angular sweep positioning

Figure 12 shows the EDS analysis performed on sample 49.1 in cross-section. In the SP1 spectrum, the carbon spectrum corresponding to the graphite substrate is shown. The lightest region in the SP2 spectrum shows copper peaks from the wear of the plasma torch electrodes that are sprayed along with the alumina. In the intermediate shade phase, the SP3 spectrum show peaks of aluminum and oxygen that corresponding to alumina of coating. The gold spectra appearing in SP1, SP2 and SP3 correspond to the gold coating that was performed in preparing the sample for microscopy.

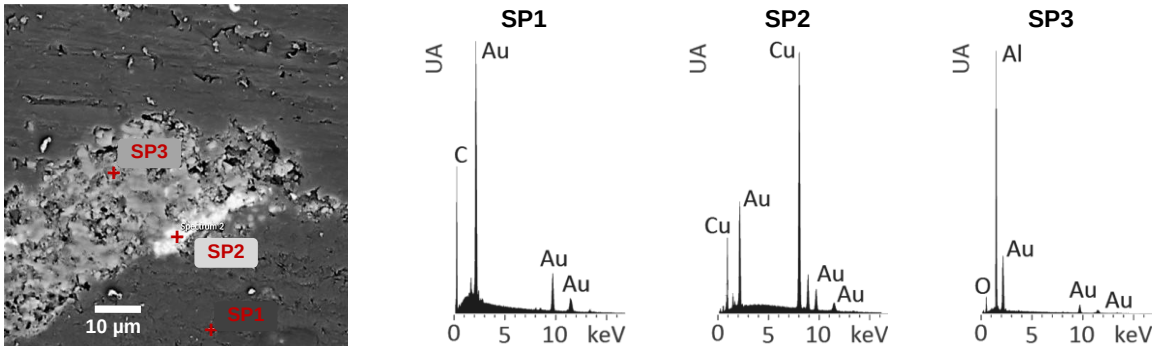

Figure 12. EDS of sample A49.1 – alumina coating on graphite substrate by using angular sweep positioning

4. CONCLUSIONS

In this work it was verified by controlling the deposition parameters it is possible to perform an alumina coating on stainless steel and graphite substrates. The deposition on graphite requires a higher concentration of energy, however, when increasing energy there is an increase in the thermal ablation process of the substrate. Thus, to obtain the coating, it is necessary to find the range of thermal spray parameters, where the deposition process occurs at a greater intensity than that of ablation for each type of substrate. It was also found that the difference in thermal coefficient between the coating material and the substrate reduces the maximum deposition time at the same region. Longer deposition times can lead to cracks as in the coatings on stainless steel performed by static positioning. With the process of rotary positioning to the deposition on stainless steel substrate, a film with uniform thickness and without cracks was obtained. This process, however, did not yield results for the graphite substrate, which needs more concentrated energy for coating. The problem was partially solved with an angular sweep positioning process applied to the sample holder. With this process, it was obtained a more homogeneous film on the carbon substrate than in the fixed positioning process, but showing accentuated undulations and irregularities in the edge region of the sample. The process showed be viable but requires improvements. It was verified in the micrographs of both substrates that the mechanical imbrication is responsible for the good adhesion observed, preliminarily, in the coatings.

5. ACKNOWLEDGEMENTS

The authors would like to thank the Brazilian Space Agency (AEB) and the National Council for Scientific and Technological Development (CNPq) for funding the research. Special thanks to Coordination of Superior Level Staff Improvement (CAPES) by National Postdoctoral Program/Capes/ITA (Grant n° 8887.360983/2019-00).

6. REFERENCES

Ando, K., Furusawa, K., Takahashi, K., & Sato, S., 2005. *Crack-healing ability of structural ceramics and a new methodology to guarantee the structural integrity using the ability and proof-test* Vol. 25, pp. 549–558.

Boulos, M. I., Fauchais, P., & Pfender, E., 1994. *Thermal Plasmas - Fundamentals and Applications.* Springer US.

Engel, T., & Kickelbick, G., 2014. "Self-healing nanocomposites from silica − polymer core − shell nanoparticles". *Polymer International*, Vol. 63, No 5, pp. 915–923.

Kim, J. I., Kim, W. J., Choi, D. J., Park, J. Y., & Ryu, W. S., 2005. "Design of a C/SiC functionally graded coating for the oxidation protection of C/C composites". *Carbon*, Vol. 43, No 8, pp. 1749–1757.

Lee, K. N., 2000. "Current status of environmental barrier coatings for Si-Based ceramics". *Surface and Coatings Technology*, Vol. 133–134, pp. 1–7.

Miranda, F. S., Caliari, F. R., Campos, T. M., Essiptchouk, A. M., & Filho, G. P., 2017. "Deposition of graded SiO2/SiC coatings using high-velocity solution plasma spray". *Ceramics International*, Vol. 43, No 18, pp. 16416–16423.

Miranda, F. S., Caliari, F. R., Campos, T. M., Leite, D. M. G., Pessoa, R. S., Essiptchouk, A. M., & Petraconi, G., 2020. "High-velocity plasma spray process using hybrid SiO2 + ZrO2 precursor for deposition of environmental barrier coatings". *Surface and Coatings Technology*, Vol. 404, No 6, pp. 126447.

Silva, R., Miranda, F., Maciel, H., & Petraconi, G., 2019a. "Development of a Thermal Spray System Using a Long Arc Plasma Torch". *Proceedings of the 25th International Congress of Mechanical Engineering - COBEM 2019*.

Silva, R., Miranda, F., Maciel, H., & Petraconi, G., 2019b. "Plasma Spray of Alumina Powder on ANSI 304 Stainless". *Proceedings of the 25th International Congress of Mechanical Engineering - COBEM 2019*.

Webster, J. D., Day, R. J., Hayes, F. H., Taylor, R., Westwood, M., Webster, J. D., & Day, R. J., 1996. "Oxidation protection for carbon fibre composites". *Journal of Materials Science*, Vol. 31, pp. 1389–1397.

7. RESPONSIBILITY NOTICE

The author(s) is (are) the only responsible for the printed material included in this paper.